Clough-Tocher interpolation of virtual sinogram in a Delaunay triangulated grid for metal artifact reduction of PET/CT images

M. Abdoli, J.R. de Jong, J. Pruim, R. A. J. O. Dierckx and H. Zaidi, *Senior Member, IEEE*

***Abstract*– Metallic implants, such as hip implants, are known to induce streaking artifacts in CT images which can cause over/underestimation of the activity uptake in CT-based attenuation corrected PET images. Hence, metal artifact reduction (MAR) of CT images is essential in order to obtain accurate quantification of PET data. The proposed MAR technique replaces the projection bins of the virtual sinogram affected by metallic implants using a 2D cubic interpolation scheme. Since removing the affected projection bins renders the sinogram grid irregular, a Delaunay triangulated gridding together with Clough-Tocher cubic interpolation, which is compatible with this irregular grid, is used to substitute the values of the affected bins. A cylindrical phantom filled with uniform activity concentration incorporating metallic inserts and 30 clinical PET-CT studies containing hip prostheses were used to assess the performance of the proposed approach. The resulting images were compared to those obtained using the built-in MAR algorithm on a Siemens mCT64 PET/CT scanner. Phantom and clinical studies showed that the proposed algorithm performed considerably better than Siemens's method in the regions corresponding to dark streaking artifacts (underestimated regions), whereas it performed equally well compared to Siemens's method in the other regions. In the underestimated regions, the proposed method increased the uptake value up to 45%, whereas the Siemens's method kept almost the same uptake as the uncorrected PET images. In the overestimated regions both methods decreased the uptake by ~45%. The phantom experiment also revealed that the proposed approach is in better agreement with the actual activity concentration compared to both the uncorrected and corrected images using Siemens's method. It can be concluded that the proposed method allows more accurate attenuation correction of PET data thus preventing misinterpretation of activity uptake in regions adjacent to metallic objects.**

This work was supported by the Swiss National Science Foundation under grant SNSF 31003A-125246, Geneva Cancer League and a research grant from Siemens Healthcare.

Mehrsima Abdoli is with the Department of Nuclear Medicine and Molecular Imaging, University Medical Center Groningen, University of Groningen, Groningen, The Netherlands (e-mail: mehrsima.abdoli@gmail.com).

Johan R. de Jong is with the Department of Nuclear Medicine and Molecular Imaging, University Medical Center Groningen, University of Groningen, Groningen, The Netherlands (e-mail: j.r.de.jong@umcg.nl).

Jan Pruim is with the Department of Nuclear Medicine and Molecular Imaging, University Medical Center Groningen, University of Groningen, Groningen, The Netherlands (e-mail: j.pruim@umcg.nl).

Habib Zaidi is with the Division of Nuclear Medicine, Geneva University Hospital, CH-1211 Geneva, Switzerland and Department of Nuclear Medicine and Molecular Imaging, University Medical Center Groningen, University of Groningen, Groningen, The Netherlands (e-mail: habib.zaidi@hcuge.ch).

I. Introduction

The presence of metallic implants in patients undergoing x-ray computed tomography (CT) scans, manifesting itself in the form of dark and bright streak artifacts, is considered to be one of the most important sources of artifacts. Depending on the implant size, these artifacts can degrade image quality in the regions surrounding the metallic object or of the whole image. CT-based attenuation correction of positron emission tomography (PET) images is the standard technique implemented on commercial PET/CT systems [1]. Following application of this procedure, metal artifacts can propagate and cause errors in the attenuation corrected PET images. The artifactual CT images lead to erroneous attenuation coefficients in some region of the generated attenuation map (μmap). This results in inaccurate quantification of the tracer uptake in the attenuation corrected PET data in the regions corresponding to the streak artifacts [2-5]. In patients with prosthetic replacements, such as hip or knee metallic implants, severe artifacts usually cause over/underestimation of the activity concentration around the prostheses. Decreased image quality impacting diagnostic accuracy has been also reported in some cases [3, 6].

After total hip replacement, local complications most likely take place including infection, mechanical loosening, prosthetic and preprosthetic fractures …etc. The diagnosis of such complications might be influenced by artifacts caused by metallic hip prosthesis [7-9]. Although moderate or minor CT streak artifacts might not affect the visual quality of the attenuation corrected PET images [10], it definitely influences the quantitative accuracy to some extent, thus leading to some bias when quantification of physiologic or pharmacokinetic processes occurring in the region of interest is desired. To enable accurate quantification of PET data, the reduction of all sources of errors and artifacts, including those generated by metallic implants, is required.

The challenging issue of metal artifact reduction (MAR) has been addressed by several approaches which can be generally categorized into sinogram- and image-based methods [11]. Sinogram-based methods manipulate the raw CT data in the sinogram space; linear interpolation of the missing sinogram bins being one of them [12, 13]. This approach detects metallic objects using a thresholding technique and then identifies the sinogram bins affected by metallic objects by forward projection of the segmented image. The affected bins are then replaced by linear interpolation of the neighbouring bins of the same projection angle. Cubic spline interpolation of the neighbouring bins is

another similar method belonging to sinogram-based approaches [14]. Jeong *et al.* applied a linear interpolation scheme on the projection data obtained from a metal-free image prepared such that the intensities of metallic regions are replaced by those of non-metallic surrounding pixels [15]. Veldkamp *et al.* performed metal object segmentation in sinogram space using a Markov random field model and replaced the corresponding values using different interpolation schemes [16]. One-dimensional spline interpolation of the projection bins of a virtual sinogram is another sinogram-based MAR technique [17].

Image-based methods are directly applied to the reconstructed image. Iterative deblurring methods [18], wavelet-based techniques [19, 20], knowledge-based approaches [21] and pattern recognition-based methods [4] are examples belonging to this category. The main complication associated with this category of methods is the fuzziness of CT numbers in the artifactual regions and the surrounding tissues, which makes the metallic object and the surrounding tissues undistinguishable and might result in lower performance.

Despite the fact that the sinogram-based methods usually result in more accurate correction [22], the practical implementation of such techniques is challenging owing to the encrypted proprietary format, manufacturer dependency and large size of the raw CT data. The advantage of our proposed MAR method is that it utilizes a virtual sinogram as an alternative to overcome the above mentioned drawbacks. It must be emphasized, however, that the smooth pattern of the sinogram has to be preserved after correction since smoothness is an inherent property of sinograms and any discontinuity and roughness can introduce extra artifacts in the reconstructed image. Therefore, the correction method has to be chosen cautiously so that the smoothness and continuity criterion will be met.

The purpose of this study is to develop a novel MAR approach by generating a smooth and continuous virtual sinogram. Since metallic hip prostheses are known to produce severe streaking artifacts and non-negligible activity concentration bias [3], the main focus of the proposed method is on reducing metallic artifacts associated with metal hip implants.

II. Materials and Methods

The MAR procedure starts by generating the virtual sinogram by forward projection of the original CT images. The projection bins affected by metallic objects are determined by segmenting the metallic objects in the original CT image using a thresholding method followed by forward projection of the segmented image. In the obtained sinogram, the projection bins having values higher than zero present the affected projection bins. To preserve the smoothness of the sinogram, a 2D cubic interpolation technique was applied to substitute the erroneous values of the affected bins. Since we omit the projection bins affected by metallic artifact from the regular grid of the sinogram, the interpolation scheme has to be performed on an irregular grid. Therefore, an irregular grid has to be defined on the unaffected projected bins over which a cubic interpolation can be performed. Delaunay triangulated grid was used for this purpose [23]. This method divides the whole data plain into triangles whose vertices are located on the data points. These triangles intersect in a common side and no data point can be inside the circumcircle of the triangles. Normal cubic interpolation method requires four data points in the grid, while in a triangulated grid only three are needed. The Clough-Tocher interpolation, which is compatible with the triangulated grid, was used in the proposed approach [24]. It divides each triangle into three sub-triangles by adding a fourth vertex on the triangle centroid. Thereafter, an interpolating cubic polynomial is formed on each sub-triangle. To define the cubic polynomials, 12 parameters (called nodal values) are required which include the function value at each vertex, first derivative of the function with respect to x and y at each vertex, and normal derivative at each mid-point of each side of the triangle. Then 12 cardinal functions of each sub-triangle are determined and multiplied by the corresponding nodal value and the results integrated to find the final value at a given point [25]. This algorithm was implemented using a MATLAB toolbox routine. The corrected sinogram is finally reconstructed using a filtered backward projection MATLAB routine to generate the corrected CT images.

The proposed algorithm was assessed using phantom and clinical studies. For the phantom experiment, a uniform cylindrical phantom containing 37 MBq of Fluorine-18 and incorporating metallic pacemakers to produce streaking artifacts was used. In addition, 30 clinical PET/CT studies of patients with metal hip prostheses (in one or both sides) were used in this study. The results were analyzed by defining 45 regions of interest (ROIs) on each dataset in the regions corresponding to bright and dark streaking artifacts as well as artifact-free regions. The mean relative difference of the tracer uptake in the uncorrected and corrected PET data was calculated for the same regions. In the case of the phantom study, the values were compared with the actual activity concentration in the phantom. The results were also compared with images corrected using the MAR method proposed by Hamill et al. which is used as a built-in function in the Siemens Syngo software [21].

III. Results

Fig. 1 shows the results of the phantom experiment. The reconstructed attenuation corrected PET images using uncorrected CT images, those corrected using the proposed MAR method and those corrected using the Siemens's MAR method are presented in this figure. Since the commercial Siemens PET-CT scanner doesn't provide corrected CT images to the user, only the uncorrected and corrected CT using the proposed MAR approach are illustrated. The bright and dark streaking artifacts in the CT image have caused overestimation and underestimation of the activity concentration in the corresponding attenuation corrected PET image (Fig. 1c). These effects are reduced by the proposed MAR method and the quality of the image is substantially improved (Fig. 1d). The Siemens's method is only successful in the overestimated regions, whereas it fails to correct for the artifacts in the underestimated regions (Fig. 1e).

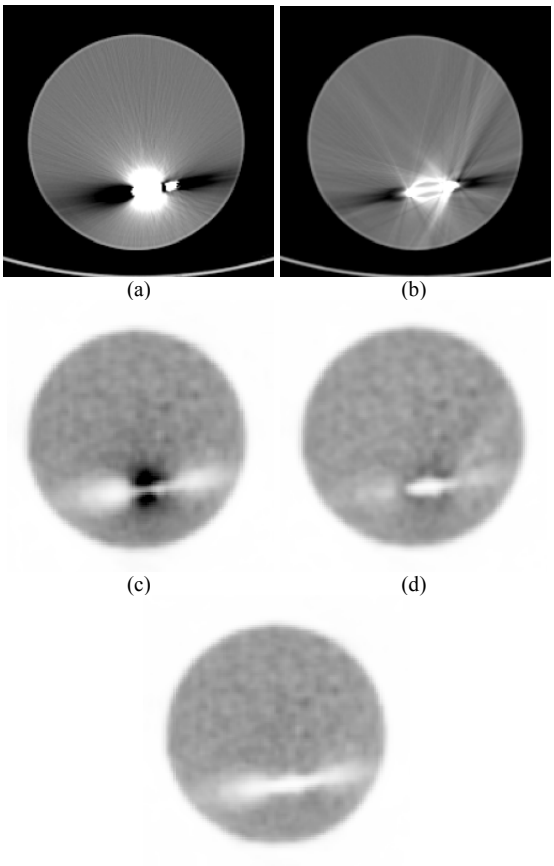

Fig. 1. Phantom study results. Uncorrected (a) and corrected (b) CT images of the phantom using the proposed MAR method. CT-based attenuation corrected PET images (c) using the image shown in (a), (d) using the image shown in (b) and (e) using the Siemens's MAR method.

Fig. 2 shows the results for CT and PET images of a clinical study. It can be observed that the proposed method decreases the artifacts in the CT image. The arrows point to a region corresponding to dark streak artifacts in the CT image. The PET image corrected for attenuation using the original CT images doesn't show high activity in the corresponding region, whereas a high uptake appears after applying the proposed algorithm. The uptake in this region remains almost similar to the uncorrected image when using Siemens's method. This is in agreement with the results of the phantom study.

Fig. 3 illustrates the results for CT and PET images of another clinical study. The arrows point to a region corresponding to bright streak artifacts in the CT image. Both methods successfully decrease the overestimated activity uptake caused by the bright streaking artifacts in the corresponding CT image.

The analysis of the 30 clinical PET-CT studies revealed that both MAR methods reduce the activity uptake values in the overestimated regions by up to ~45%. In the underestimated regions though, only the proposed method increases the values up to ~45%, while the Siemens's MAR approach keeps almost the same values in these regions. The uptake values remain similar to the uncorrected PET data for both techniques in the unaffected regions (Table I).

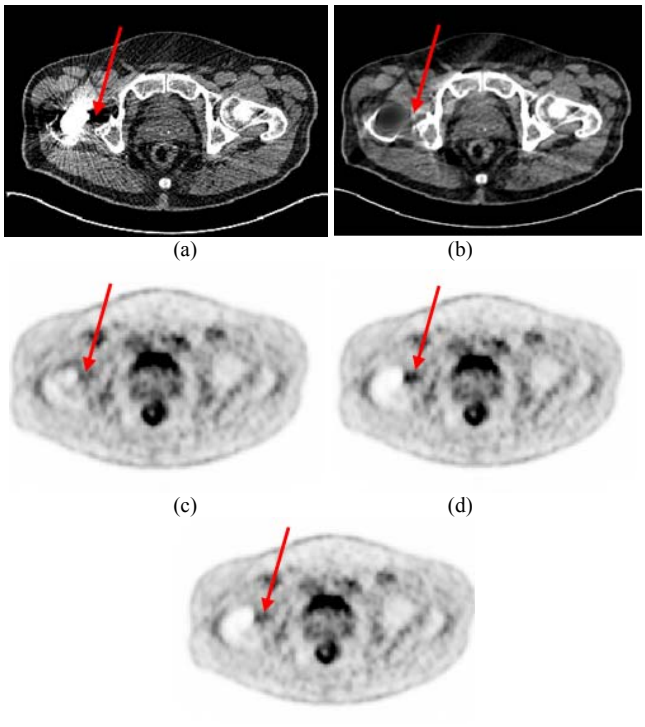

Fig. 2. A clinical PET-CT study showing (a) uncorrected and (b) corrected CT images using the proposed MAR method. (c),(d) Attenuation corrected PET images using (a) and (b), respectively. (e) Attenuation corrected PET data using Siemens's MAR method. The arrows point to a dark streaking artifact region in the uncorrected CT image and the corresponding region in the other images.

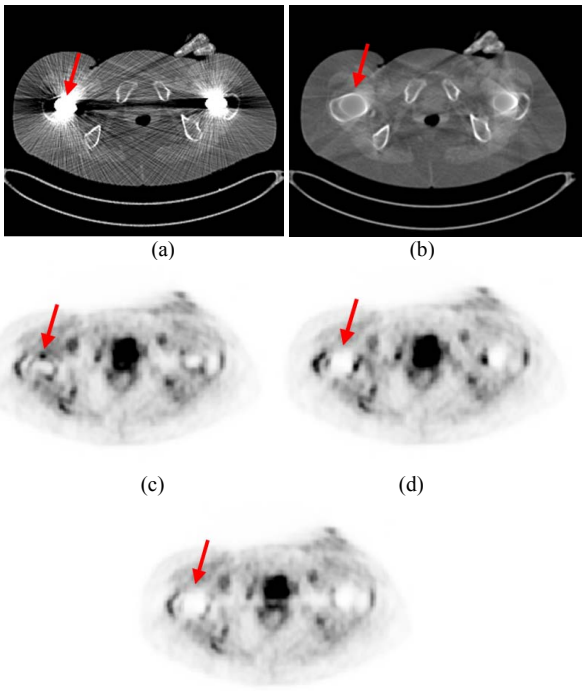

Fig. 3. Another clinical PET-CT study showing (a) uncorrected and (b) corrected CT images using the proposed MAR method. (c),(d) Attenuation corrected PET images using (a) and (b), respectively. (e) Attenuation corrected PET data using Siemens's MAR method. The arrows point to a bright streaking artifact region in the uncorrected CT image and the corresponding region in the other images.

TABLE I. MEAN RELATIVE DIFFERENCE (%) BETWEEN THE ACTUAL ACTIVITY OF THE PHANTOM IN DIFFERENT REGIONS AND THE UNCORRECTED CLINICAL PET DATA AS WELL AS THOSE CORRECTED USING THE PROPOSED AND SIEMENS'S MAR METHODS.

Regions	Datasets		
	Uncorrected	Proposed MAR	Siemens's MAR
Overestimated	127.95±35.7	25.49±9.5	-20.96±9.2
Underestimated	-82.21±4.5	-45.76±11.9	-81.81±5.5
Unaffected	-2.48±3.5	-5.73±3.4	-5.47±3.4

IV. DISCUSSION

The phantom study revealed that the proposed MAR algorithm results in visually acceptable PET images. The black and white regions in Fig. 1c represent over- and under-estimation of activity concentration since the phantom is filled with uniform activity. These artifacts are caused by the bright and dark streaks shown in Fig. 1a. It can be seen that the proposed method has successfully suppressed erroneous estimations around the metallic object (Fig. 1b). However, Siemens' method fails to correct the underestimation (white regions around the metallic object), although it corrects appropriately the overestimated regions.

The quantitative analysis further demonstrates that the estimated activity concentration approaches the actual activity concentration within the phantom when using the proposed MAR method. Although there is a slight difference between the corrected and actual activity concentration (Table I), this difference was reduced from over 120% in the overestimated regions to less than 30% and from about -80% to -45% in the underestimated regions. On the other hand, Siemens' MAR method over-corrects the activity concentration (the difference decreases from ~120% to -20%) in the overestimated regions. However, the method doesn't seem to handle appropriately the underestimated regions where the activity concentration remains similar to the uncorrected data. In the unaffected regions, both methods keep the original uptake unchanged, which is desirable.

The clinical PET/CT studies had a similar trend. In the underestimated regions, the uncorrected PET image has no significant uptake in the corresponding region (Fig. 2), which corresponds to dark streaking artifact regions in the CT image. After correction using the proposed MAR, a high activity uptake is visible in the same region, while the image corrected using Siemens' MAR technique remains unchanged. In Fig. 3, while the uncorrected PET image shows a high activity uptake in the region corresponding to bright streaking artifacts in the CT image, both corrected PET images have low uptake in the same region, which confirms that both MAR methods perform similarly in overestimated regions. These results are in agreement with the phantom study.

It must be emphasized that in the absence of gold standard for the clinical studies, it is challenging to draw general conclusions with respect to the relevance of MAR in clinical setting [26]. Nevertheless, the phantom study revealed that the activity concentration in regions corresponding to bright and dark streaking artifacts best match the actual activity concentration after applying the proposed MAR technique. This supports the opinion that the clinical results obtained using the proposed method are also more reliable than the uncorrected data as well as those obtained using Siemens' method.

V. CONCLUSION

We presented an approach for reduction of artifacts in PET/CT images caused by metallic hip prostheses allowing the generation of a smooth and continuous sinogram. The performance of the proposed method in regions corresponding to bright streaking artifacts and artifact-free regions is similar to the method proposed by Hamill *et al.* [21] implemented on Siemens PET/CT scanners. However, the proposed method is superior in the regions corresponding to dark streaking artifacts. This approach makes CT-based attenuation correction of PET images more accurate and prevents misinterpretation of activity uptake in some regions which might be biased due to the propagation of bright and dark streaking artifacts of CT images. The proposed method increases both the quantitative accuracy and the diagnostic image quality of PET images when compared to Siemens' method.

ACKNOWLEDGEMENTS

This work was supported the Swiss National Science Foundation under grant SNSF 31003A-125246, Geneva Cancer League and a research grant from Siemens Healthcare.

REFERENCES

[1] H. Zaidi and B. Hasegawa, "Determination of the attenuation map in emission tomography.," *J Nucl Med.,* vol. 44, pp. 291-315, 2003.

[2] E. M. Kamel, C. Burger, A. Buck, G. K. von Schulthess, and G. W. Goerres, "Impact of metallic dental implants on CT-based attenuation correction in a combined PET/CT scanner," *Eur Radiol,* vol. 13, pp. 724-8, 2003.

[3] G. W. Goerres, S. I. Ziegler, C. Burger, T. Berthold, G. K. Von Schulthess, and A. Buck, "Artifacts at PET and PET/CT caused by metallic hip prosthetic material," *Radiology,* vol. 226, pp. 577-84, 2003.

[4] J. A. Kennedy, O. Israel, A. Frenkel, R. Bar-Shalom, and H. Azhari, "The reduction of artifacts due to metal hip implants in CT-attenuation corrected PET images from hybrid PET/CT scanners," *Med Biol Eng Comput,* vol. 45, pp. 553-62, 2007.

[5] C. Lemmens, M. L. Montandon, J. Nuyts, O. Ratib, P. Dupont, and H. Zaidi, "Impact of metal artefacts due to EEG electrodes in brain PET/CT imaging," *Phys Med Biol,* vol. 53, pp. 4417-29, 2008.

[6] S. I. Heiba, J. Luo, S. Sadek, E. Macalental, A. Cacavio, G. Rosen, and H. A. Abdel-Dayem, "Attenuation-Correction Induced Artifact in F-18 FDG PET Imaging Following Total Knee Replacement," *Clin Positron Imaging,* vol. 3, pp. 237-239, 2000.

[7] H. J. Griffiths, D. R. Priest, D. M. Kushner, and D. Kushner, "Total hip replacement and other orthopedic hip procedures," *Radiol Clin North Am,* vol. 33, pp. 267-87, Mar 1995.

[8] C. Cyteval, V. Hamm, M. P. Sarrabere, F. M. Lopez, P. Maury, and P. Taourel, "Painful infection at the site of hip prosthesis: CT imaging," *Radiology,* vol. 224, pp. 477-83, 2002.

[9] K. D. Stumpe, H. P. Notzli, M. Zanetti, E. M. Kamel, T. F. Hany, G. W. Gorres, G. K. von Schulthess, and J. Hodler, "FDG PET for differentiation of infection and aseptic loosening in total hip replacements: comparison with conventional radiography and three-phase bone scintigraphy," *Radiology,* vol. 231, pp. 333-41, 2004.

[10] C. Nahmias, C. Lemmens, D. Faul, E. Carlson, M. Long, T. Blodgett, J. Nuyts, and D. Townsend, "Does reducing CT artifacts from dental implants influence the PET interpretation in PET/CT studies of oral cancer and head and neck cancer?," *J Nucl Med,* vol. 49, pp. 1047-52, 2008.

[11] H. Zaidi, M. L. Montandon, and A. Alavi, "Advances in attenuation correction techniques in PET," *PET Clin.,* vol. 2, pp. 191-217, 2007.
[12] W. A. Kalender, R. Hebel, and J. Ebersberger, "Reduction of CT Artifacts Caused by Metallic Implants," *Radiology,* vol. 164, pp. 576-577, 1987.
[13] M. Yazdi, L. Gingras, and L. Beaulieu, "An adaptive approach to metal artifact reduction in helical computed tomography for radiation therapy treatment planning: experimental and clinical studies," *Int J Radiat Oncol Biol Phys,* vol. 62, pp. 1224-31, 2005.
[14] M. Bazalova, L. Beaulieu, S. Palefsky, and F. Verhaegena, "Correction of CT artifacts and its influence on Monte Carlo dose calculations," *Med Phys,* vol. 34, pp. 2119-32, 2007.
[15] K. Y. Jeong and J. B. Ra, "Metal Artifact Reduction Based on Sinogram Correction in CT," in *IEEE Nuclear Science Symposium Conference Record (NSS/MIC)*, Orlando, FL 2009, pp. 3480 - 3483
[16] W. J. Veldkamp, R. M. Joemai, A. J. van der Molen, and J. Geleijns, "Development and validation of segmentation and interpolation techniques in sinograms for metal artifact suppression in CT," *Med Phys,* vol. 37, pp. 620-8, 2010.
[17] M. Abdoli, M. R. Ay, A. Ahmadian, and H. Zaidi, "A virtual sinogram method to reduce dental metallic implant artefacts in computed tomography-based attenuation correction for PET," *Nucl Med Commun,* vol. 31, pp. 22-31, 2010.
[18] D. D. Robertson, J. Yuan, G. Wang, and M. W. Vannier, "Total hip prosthesis metal-artifact suppression using iterative deblurring reconstruction," *J Comput Assist Tomogr,* vol. 21, pp. 293-8, 1997.
[19] S. Zhao, D. D. Robertson, G. Wang, B. Whiting, and K. T. Bae, "X-ray CT metal artifact reduction using wavelets: an application for imaging total hip prostheses," *IEEE Trans Med Imaging,* vol. 19, pp. 1238-47, 2000.
[20] S. Zhao, K. T. Bae, B. Whiting, and G. Wang, "A wavelet method for metal artifact reduction with multiple metallic objects in the field of view," *J X-Ray Sci Technol,* vol. 10, pp. 67-76, 2002.
[21] J. J. Hamill, R. C. Brunken, B. Bybel, F. P. DiFilippo, and D. D. Faul, "A knowledge-based method for reducing attenuation artefacts caused by cardiac appliances in myocardial PET/CT," *Phys Med Biol,* vol. 51, pp. 2901-18, 2006.
[22] C. Lemmens, D. Faul, and J. Nuyts, "Suppression of metal artifacts in CT using a reconstruction procedure that combines MAP and projection completion," *IEEE Trans Med Imaging,* vol. 28, pp. 250-260, 2009.
[23] P. B. Delaunay, "Sur la sphère vide " *Bulletin of Academy of Sciences of the USSR,* vol. 6, pp. 793-800, 1934.
[24] R. Clough and J. Tocher, "Finite element stiffness matrices for analysis of plates in blending," in *Proceedings of Conference on Matrix Methods in Structural Analysis.*, Wright-Patterson A.F.B., Ohio, 1965, pp. 515-545.
[25] P. Lancaster and K. Salkauskas, Curve and Surface Fitting, an introduction. London: Academic Press, 1986.
[26] M. Abdoli, M. Ay, A. Ahmadian, R. Dierckx, and H. Zaidi, "Reduction of dental filling metallic artefacts in CT-based attenuation correction of PET data using weighted virtual sinograms optimized by a genetic algorithm.," *Med Phys,* vol. 37, pp. 6166-6177, 2010.